Biologia, Bratislava, **57/Suppl. 11:** 163—170, 2002

Mechanism of porcine pancreatic α-amylase: inhibition of amylose and maltopentaose hydrolysis by various inhibitors

Véronique Desseaux[1]*, Roger Koukiekolo[1], Yann Moreau[2], Marius Santimone[1] & Guy Marchis-Mouren[1]

[1]*IMRN, Institut Méditerranéen de Recherche en Nutrition, Faculté des Sciences et Technique de St Jérome, Université d'Aix-Marseille, Av. Esc. Normandie-Niemen case 342, F-13397 Marseille cedex 20, France; fax : ++ 33 4 91 28 84 40, e-mail: veronique.desseaux@univ.u-3mrs.fr*
[2]*IRD, Institut de Recherche pour le Développement, Gamet c/o CEMAGREF BP 5095, F-34033 Montpellier cedex 1, France*

Desseaux, V., Koukiekolo, R., Moreau, Y., Santimone, M. & Marchis-Mouren, G., Mechanism of porcine pancreatic α-amylase: inhibition of amylose and maltopentaose hydrolysis by various inhibitors. Biologia, Bratislava, **57/Suppl. 11:** 163—170, 2002; ISSN 0006-3088.

The effect of the pseudotetrasaccharide inhibitor acarbose, α-, β- and γ-cyclodextrins and the *Phaseolus* protein inhibitor α-AI on amylose and maltopentaose porcine pancreatic α-amylase (PPA)-catalysed hydrolysis was studied. Statistical analysis of the kinetic data was performed. Acarbose is a strong inhibitor (K_{1i} = 1.6 μM for amylose and 3 μM for maltopentaose). The inhibition is of the mixed noncompetitive type involving abortive complexes. α-, β- and γ-cyclodextrins are much weaker inhibitors (K_{1i} = 7, 1.2 and 3 mM, respectively with amylose and 7, 2.5 and 3.1 mM, respectively for maltopentaose). The inhibition of amylose hydrolysis is competitive while the inhibition of maltopentaose hydrolysis is, as above, mixed noncompetitive. The *Phaseolus* protein α-AI is a strong inhibitor of both amylose and maltopentaose hydrolysis. However, the inhibition differs from the ones described above, in that a preincubation period of the inhibitor with PPA is required. However the same general equation applies and the inhibition is mixed noncompetitive. Aside from the inhibition of amylose hydrolysis by cyclodextrins, the other examples of inhibition, whatever the inhibitor used, are of the mixed noncompetitive type indicating that one (or two) secondary carbohydrate binding site(s) in addition to the active site participate(s) in the amylolytic process. X-ray studies of the crystallized amylase-inhibitor/substrate complex show secondary (accessory) carbohydrate binding sites in addition to the active site. These binding sites are very likely the same as those kinetically determined; they might play a role either at the substrate entrance or at the product exit and they might also participate in displacement of the amylose chain in the multiple attack mechanism.

Key words: porcine pancreatic α-amylase, inhibition kinetics, maltopentaose, acarbose, cyclodextrin, *Phaseolus vulgaris*.

* Corresponding author

Abbreviations: PPA, porcine pancreatic α-amylase; HPA, human pancreatic α-amylase; DP, degree of polymerization; α-CD, α-cyclodextrin or cyclohexaamylose; β-CD, β-cyclodextrin or cycloheptaamylose; γ-CD, γ-cyclodextrin or cyclooctaamylose; α-AI, *Phaseolus* protein inhibitor.

Introduction

α-Amylases (EC 3.2.1.1) catalyse the hydrolysis of internal α-(1→4)-glycoside linkages in starch components and related derivatives. This retaining enzymes belong to glycosyl hydrolase family no. 13 (McCarter & Withers, 1994; Gottschalk et al., 1998). In the case of porcine pancreatic α-amylase (PPA), according to the multiple attack hypothesis, PPA (E) remains bound, after the first endoglycosidic attack, to the new reducing end of the glycoside half chain and switches to the exoglucosidase mode of action, releasing several maltose molecules before the ES complex is dissociated (Robyt & French, 1970). This highly unusual mechanism has not yet been properly elucidated, nor have the functions of several structural features of PPA yet been explained.

α-Amylases are present in Archaea, Procarya and Eucarya species (Janecek, 1994). Although very little sequence homology has been found to exist between them, their three-dimensional structures are all very similar (Jespersen et al., 1991). The 496-amino-acid sequence of porcine pancreatic α-amylase has been determined (Pasero et al., 1986). The protein is composed of a large domain (residues 1-405) featuring a central $(\beta/\alpha)_8$ barrel and a compact C-terminal domain (residues 406-496) with an γ-crystallin topology (Buisson et al., 1987; Qian et al., 1993). The active site, a long deep polysaccharide-binding cleft, crosses the C-terminal end of the $(\beta/\alpha)_8$ barrel (Larson et al., 1994). The structure of the pseudotetrasaccharide complex – which mimics the transition state with crystalline PPA – has been determined by X-ray crystallography, and shows that acarbose occupies the active site (Gilles et al., 1996). A secondary surface carbohydrate-binding site has been detected in the Aα_7Aα_8 region facing the C-terminal domain segment between β_9 and β_{10} in the 4,4'-dithio-α-maltotrioside-PPA complex (Qian et al., 1997). Two secondary binding sites have also been observed in the maltopentaose-PPA complex (Qian et al., 1995).

Phaseolus protein inhibitor (α-AI) is a 56 kDa dimeric glycoprotein (Le Berre-Anton et al. 1997). X-ray analysis, at 0.18 nm resolution, of the α-AI co-crystallised with PPA showed the existence of a complex with a 1:2 stoechiometry (α-AI/PPA). Two hairpin loops extending out from the jelly-roll fold of a monomer, interact directly with the active-site region of PPA, and the inhibitor fills the whole substrate-docking region of the enzyme (Bompard-Gilles et al., 1996).

X-ray analysis of the crystalline PPA-α-cyclodextrin complex showed the presence of three binding sites by difference-Fourier maps (Larson et al., 1994): one is located near the center of the long polysaccharide-binding cleft; another is at the extremity of this cleft and the third (accessory site) is at the edge of the protein and is quite distinct from the cleft. The use of cyclodextrins as inhibitors is of interest as these molecules are chemically identical to amylose and maltodextrins, and their cyclic structure, especially that of β-cyclodextrin, resembles the six-glycosyl-residue turn in the amylose helix.

In order to understand further the role of these sites, inhibition kinetics have been carried out using substrate-analogues: acarbose (Al Kazaz et al., 1996, 1998), cyclodextrins (Koukiekolo et al., 2001) and the red bean lectin-like amylase inhibitors (Koukiekolo et al., 1999).

In the present study, the inhibition of amylose and maltopentaose hydrolysis by the various above-mentioned inhibitors was investigated. The inhibition processes are compared, especially those between substrate-analogues and the lectin-like inhibitor.

Material and methods

Materials

PPA was purified from porcine pancreas (Granger et al., 1975). The amylase concentration was determined by absorbance at 280 nm (Al Kazaz et al., 1996). Acarbose (*O*-4", 6"-dideoxy-4-[[4,5,6-trihydroxy-3-hydroxymethyl-2-cyclohexen-1yl]amino]-α-D-glucopyranosyl-(1→4)-*O* − α-D-glucopyranosyl-(1→4)-D-glucose) was supplied by Bayer Pharma, France. α- β- and γ-cyclodextrins were from Sigma. The α-amylase inhibitor α-AI was isolated from kidney bean (*Phaseolus vulgaris* cv Tendergreen) seeds (Le Berre-Anton et al., 1997). Amylose (type III from potato) was from Sigma. Its molar mass (794 kDa) was calculated from the degree of polymerization, DP 4900, determined by performing intrinsic viscosimetry (Chen et al., 1997). Amylose (DP

18) was from Hayashibara Biochemical Laboratories, Inc. (Okayama, Japan). The reduction method is as described by Al Kazaz et al. (1996). Maltopentaose, maltotriose, maltose and neocuproine were from Sigma. Analysis of acarbose, maltopentaose and cyclodextrins by high-performance anion-exchange chromatography with pulsed amperometric detection showed no significant impurities.

Kinetics

Kinetic experiments were performed at 30 °C in 20 mM sodium phosphate buffer pH 6.9 containing 6 mM NaCl and 1 mM sodium azide. Substrate and inhibitor were mixed together and the reaction was initiated by adding amylase. No preincubation was required except for the *Phaseolus* inhibitor (2 h). More than 10 concentrations of each substrate, amylose (either 10.6-171 nM or 8.4-136 $\mu g \cdot mL^{-1}$), reduced average DP 18 maltodextrin (10–400 μM) and maltopentaose (25–500 μM) were used. The amylase concentration was 0.3 nM for amylose hydrolysis and 1 nM for maltopentaose hydrolysis. The acarbose concentrations were 0.15–1.8 μM, those of α-cyclodextrin were 1–14 mM and those of β- and γ-cyclodextrin were 1–5 mM, those of α-AI were 48–70 nM for amylose hydrolysis and 100–500 nM for maltopentaose hydrolysis. In the case of amylose and reduced DP 18 maltodextrin hydrolysis, the reducing power was determined according to Dygert et al. (1965). The maltotriose and maltose resulting from the maltopentaose hydrolysis were analysed by performing high-performance anion-exchange chromatography with pulsed amperometric detection; Dionex DX 500 chromatography HPLC system equipped with a GP 50 gradient pump and an ED 40 electrochemical detector was used as previously described (Al Kazaz et al., 1998). The initial velocity was determined from the slope, as calculated by linear regression, of the linear part of the kinetic curves giving either the number of hydrolysed bonds or the changes in product and substrate concentration with time. All the experiments were repeated three to four times.

Statistical analysis

Statistical analyses were performed using either the REG, NLIN or GLM procedure from the SAS/STAT Software package (SAS Institute Inc., 1989).

Results and discussion

Inhibition by acarbose and α- β- and γ-cyclodextrins

The effects of the saccharidic inhibitors on PPA-catalysed amylose and maltopentaose hydrolysis were studied. The initial velocity v was measured at various substrate concentrations S and in the presence of the indicated inhibitor amount I. Acarbose and α- β- and γ-cyclodextrins inhibit both amylose and maltopentaose hydrolysis.

In order to determine which inhibition model applies, i.e. whether the inhibition is of the competitive, noncompetitive or uncompetitive type and whether it occurs in the steady state or at rapid equilibrium, a general initial velocity equation is necessary for the statistically-analysed data. Let us examine first the two simplest models in the case of noncompetitive inhibition, either of random type or involving abortive complexes (Scheme 1).

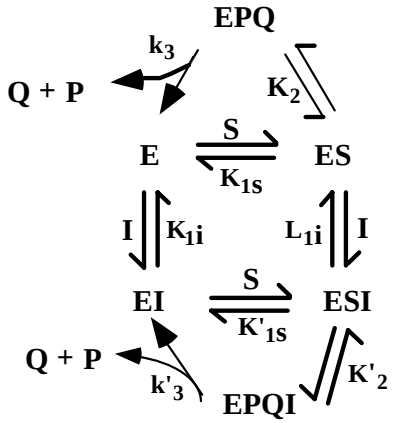

Model of random type noncompetitive inhibition

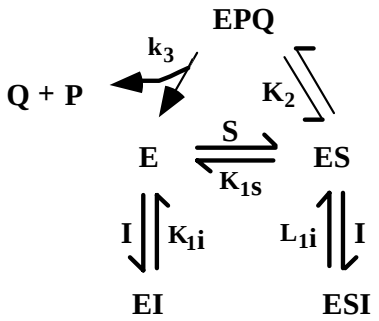

Model involving abortive complexes noncompetitive inhibition

Scheme 1. E, S, I, P and Q are the enzyme, the substrate, the inhibitor and the products, respectively; K, L are dissociation constants; k and k' are rate constants.

Table 1. Inhibition equations.[a]

Inhibitor	Substrate	Equation		Inhibition type Enzyme inhibitor complexes
Acarbose	Amylose	$v/[\mathrm{E}]_0 = \dfrac{k_{\mathrm{cat}}[\mathrm{S}]}{K_m\left(1+\dfrac{1}{K_{1\mathrm{i}}}[\mathrm{I}]+\dfrac{1}{K_{1\mathrm{i}}K_{2\mathrm{i}}}[\mathrm{I}]^2\right)+[\mathrm{S}]\left(1+\dfrac{1}{L_{1\mathrm{i}}}[\mathrm{I}]+\dfrac{1}{L_{1\mathrm{i}}L_{2\mathrm{i}}}[\mathrm{I}]^2\right)}$	(2)	Mixed noncompetitive EI, ESI, EI_2, ESI_2
	rDP18 Maltopentaose	$v/[\mathrm{E}]_0 = \dfrac{k_{\mathrm{cat}}[\mathrm{S}]}{K_m\left(1+\dfrac{1}{K_{1\mathrm{i}}}[\mathrm{I}]\right)+[\mathrm{S}]\left(1+\dfrac{1}{L_{1\mathrm{i}}}[\mathrm{I}]\right)}$	(1)	Mixed noncompetitive EI, ESI
Cyclodextrins (α-,β-,γ-)	Amylose	$v/[\mathrm{E}]_0 = \dfrac{k_{\mathrm{cat}}[\mathrm{S}]}{K_m\left(1+\dfrac{1}{K_{1\mathrm{i}}}[\mathrm{I}]\right)+[\mathrm{S}]}$	(3)	Competitive EI
	Maltopentaose	$v/[\mathrm{E}]_0 = \dfrac{k_{\mathrm{cat}}[\mathrm{S}]}{K_m\left(1+\dfrac{1}{K_{1\mathrm{i}}}[\mathrm{I}]\right)+[\mathrm{S}]\left(1+\dfrac{1}{L_{1\mathrm{i}}}[\mathrm{I}]\right)}$	(1)	Mixed noncompetitive EI, ESI
Phaseolus, α-AI	Amylose Maltopentaose	$v/[\mathrm{E}]_0 = \dfrac{k_{\mathrm{cat}}[\mathrm{S}]}{K_m(1+\dfrac{1}{K_{2\mathrm{i}}}[\mathrm{I}]^2)+[\mathrm{S}](1+\dfrac{1}{L_{2\mathrm{i}}}[\mathrm{I}]^2)}$	(4)	Mixed noncompetitive EI_2, ESI_2

[a] $K_{1\mathrm{i}}$, $K_{2\mathrm{i}}$, $L_{1\mathrm{i}}$ and $L_{2\mathrm{i}}$ are the dissociation constants of the inhibitor containing complexes EI, EI_2, ESI and ESI_2, respectively.

When noncompetitive inhibition is of the random type, the inhibitor cannot bind to the active site of the enzyme. Actually, the binding of S gives an active ES complex, which means that S is bound to the active center. Consequently, the inhibitor cannot further bind to the active center, as it is already occupied. In the present study, the random-type model can be ruled out on two experimental grounds.

a) Both acarbose and the cyclodextrins are hydrolysed under certain conditions by PPA; this indicates that the inhibitor molecule can occupy the active site (KONDO et al., 1990; ABDULLAH et al., 1966). b) X-ray crystallographic analysis of the PPA-acarbose complex (GILLES et al. 1996), the PPA-α-CD complex (LARSON et al., 1994) and of the PPA-α-AI complex (BOMPARD-GILLES et al., 1996) show that one inhibitor molecule is present at the active site. The first molecule I which binds to PPA (E) is bound to the active center which agrees with the abortive-type model. This type of inhibition can be assumed to occur either in the steady state or at rapid equilibrium. (Indeed the initial velocity calculated either at equilibrium or in the steady state using the King and Altman rules (KING & ALTMAN, 1956) gives linear double reciprocal plots $1/v$ vs. $1/[S]$ which are consistent with our data.)

Whichever hypothesis is adopted, the initial velocity fits the following equations:

$$v/[E]_0 = \frac{k_{cat}[S]}{K_m\left(1+\frac{1}{K_{1i}}[I]\right)+[S]\left(1+\frac{1}{L_{1i}}[I]\right)} \quad (1)$$

Equation (1) applies if we assume that only one molecule of I is bound to the enzyme or to the enzyme-substrate complex (two abortive complexes EI and ESI).

$$v/[E]_0 = k_{cat}[S]\Big/\left[K_m\left(1+\frac{1}{K_{1i}}[I]+\frac{1}{K_{1i}K_{2i}}[I]^2\right)+[S]\left(1+\frac{1}{L_{1i}}[I]+\frac{1}{L_{1i}L_{2i}}[I]^2\right)\right] \quad (2)$$

Equation (2) applies when two molecules of inhibitor are involved in the binding process (two abortive complexes EI_2 and ESI_2; AL KAZAZ et al., 1996).

For the statistical analysis of the kinetic data, four types of initial velocity equations were considered. When PPA is inhibited by acarbose and when amylose is substrate, equation (2) (Tab. 1) fits better. The molecular inhibitor-containing complexes are EI, EI_2, ESI and ESI_2 suggesting two secondary (accessory) binding sites. When maltopentaose is the substrate, equation (1) fits better, only EI and ESI enzyme-inhibitor complexes are present, suggesting that only one secondary binding site is needed for PPA-catalysed maltopentaose hydrolysis. In the case of inhibition by cyclodextrins, when amylose is substrate, equation (1) in which $1/L_{1i} = 0$ fits better and a single enzyme-inhibitor complex is observed, EI [Tab. 1, equation (3)]; when maltopentaose is substrate, equation (1) in which $1/L_{1i} \neq 0$ fits better, two enzyme-inhibitor complexes EI and ESI are present.

As expected the Lineweaver-Burk plots obtained when acarbose and cyclodextrins inhibit amylose and maltopentaose hydrolysis are straight lines (not shown). The secondary plots drawn from the acarbose/amylose reciprocal plot are parabolic lines (not shown) which confirms that two acarbose molecules are bound to PPA. In contrast the secondary plot drawn from the CD-amylose primary plot and from the acarbose-maltopentaose and CD-maltopentaose primary plots are linear (one inhibitor molecule bound to PPA).

The inhibition can also be described by the dissociation constant values of the inhibitor-enzyme complexes (Tab. 2). The acarbose inhibition constants are in the micromolar range while those obtained when cyclodextrin is inhibitor are in the millimolar range. Acarbose is thus a stronger inhibitor than cyclodextrins.

Inhibition by α-AI

The inhibition mechanism differs from the one observed with the saccharidic inhibitors discussed above, since a preincubation period is required between PPA and α-AI for the inhibition to take place. In our experiments α-AI and PPA were incubated for 2 h before the start of the reaction by adding the substrate (no preincubation effect was observed with acarbose or with CDs). The prolonged incubation period ensures that complete equilibrium is reached between the enzyme, the inhibitor and the enzyme-inhibitor complex and it allows us to postulate that the mechanism is at equilibrium.

The general equation (2) (Tab. 1) was considered and the data fit equation (4) better, in which the [I] term has been disregarded:

$$v/[E]_0 = \frac{k_{cat}[S]}{K_m(1+\frac{1}{K_{2i}}[I]^2)+[S](1+\frac{1}{L_{2i}}[I]^2)} \quad (4)$$

Table 2. Inhibition constants.[a]

Inhibitor	Substrate	K_{1i}	K_{2i} μM	L_{1i} μM	L_{2i} μM
Acarbose	Amylose	1.6 ± 0.7 μM	0.43 ± 0.04	1.6 ± 0.1	0.4 ± 0.1
	rDP18	0.8 ± 0.3 μM		0.22 ± 0.03	
	Maltopentaose	3 ± 0.6 μM		0.62 ± 0.2	
α-CD	Amylose	7 ± 0.7 mM			
	Maltopentaose	7.0 ± 2 mM	ns	ns	ns
β-CD	Amylose	1.2 ± 0.2 mM			
	Maltopentaose	2.5 ± 1.1 mM	ns	ns	ns
γ-CD	Amylose	3 ± 0.2 mM			
	Maltopentaose	3.1 ± 0.7 mM	ns	ns	ns
Inhibitor	Substrate		$\overline{K}_{2i}$ μM^2		$\overline{L}_{2i}$ μM^2
α-AI	Amylose	ns	2×10^{-9}	ns	4×10^{-9}
	Maltopentaose	ns	0.05×10^{-6}		0.13×10^{-6}

[a] K_{1i}, K_{2i}, L_{1i} and L_{2i} are dissociation constants of the inhibitor containing complexes EI, EI_2, ESI and ESI_2, respectively. In the case of α-AI, $\overline{K}_{2i}$ and $\overline{L}_{2i}$ are apparent dissociation constants. ns: no-significant.

This suggests that $1/K_{1i}$ and $1/L_{1i}$ values are close to 0, indicating that EI and ESI complexes are in negligible amount, while EI_2 and ESI_2 are the major enzyme-inhibitor complexes present. It may be that EI, which is formed during the preincubation period, is very rapidly converted into ESI, EI_2 and ESI_2 when S is added and ESI converted into ESI_2. $\overline{K}_{2i}$ and $\overline{L}_{2i}$ are apparent dissociation constants of EI_2 and ESI_2, respectively, in the $E + 2I \rightleftarrows EI_2$ and $E + S + 2I \rightleftarrows ESI_2$ equilibria, respectively. Let us notice that under some conditions, the E_2I complex is formed (Bompard-Gilles et al., 1996). The inhibition is mixed noncompetitive. As expected the Lineweaver-Burk plots of amylose and maltopentaose hydrolysis inhibition were quite similar. These primary plots give straight lines in both cases (not shown). The secondary plots, plotting both the slope (s) and the vertical axis intercept (i) versus the inhibitor concentration produced parabolic lines (not shown) as resulting from statistical analysis. This confirms that under our conditions, two molecules of inhibitor bind to both the free enzyme and the ES complex.

General discussion

The statistical analysis of the kinetic data reveals that the inhibitory mechanism depends on both inhibitor and substrate used, the underlying inhibitory mechanism being obviously quite different between saccharidic and protein inhibitors. Actually upon binding of α-AI, the structural changes observed are very different from those induced by acarbose (Qian et al., 1994); with α-AI, conformational changes are observed both at the active site and in several other regions of PPA (Bompard-Gilles et al., 1996). An extended protein-protein interface can be observed. Those regions might correspond to the secondary binding sites kinetically determined. The slow inactivation of PPA by α-AI very likely results from the time necessary for the conformational changes to take place (equilibrium). From these kinetic studies, the difference is that in the PPA-α-AI2 (EI_2) and PPA-α-AI2S (ESI_2) in the EI_2 and ESI_2 abortive complexes, α-AI occupies the active site and S is bound to a secondary binding site. In contrast acarbose is present at the active site in the complexes EI, ESI, EI_2 and ESI_2 and S never binds to a secondary site. In the α-AI experiment, the binding of S at a secondary site induced by α-AI very likely results from conformational changes. Interaction regions between α-AI and HPA (whose structure is quite close to PPA) have been determined by X-ray analysis (Nahoum et al., 2000); they might participate in the binding of the amylose chain to PPA, thus the blocking of this region should inhibit PPA activity by forming abortive complexes. Those results agree with the molecular modelling studies

of PPA with amylose fragments (Casset et al., 1995).

Acknowledgements

We are very grateful to Claude Villard for maltosaccharide analyses.

References

Abdullah, M., French, D. & Robyt, J. F. 1966. Multiple attack by α-amylases. Arch. Biochem. Biophys. **114:** 595–598.

Al Kazaz, M., Desseaux, V., Marchis-Mouren, G., Payan, F., Forest, E. & Santimone, M. 1996. The mechanism of porcine pancreatic α-amylase. Kinetic evidence for two additional carbohydrate-binding sites. Eur. J. Biochem. **241:** 787–796.

Al Kazaz, M., Desseaux, V., Marchis-Mouren, G., Prodanov, E. & Santimone, M. 1998. The mechanism of porcine pancreatic α-amylase. Inhibition of maltopentaose hydrolysis by acarbose, maltose and maltotriose. Eur. J. Biochem. **252:** 100–107.

Bompard-Gilles, C., Rousseau, P., Rougé, P. & Payan, F. 1996. Substrate mimicry in the active center of a mammalian α-amylase: structural analysis of an enzyme-inhibitor complex. Structure **4:** 1441–1452.

Buisson, G., Duée, E., Haser, R. & Payan, F. 1987. Three-dimensional structure of porcine pancreatic α-amylase at 2.9 Å resolution. Role of calcium in structure and activity. EMBO J. **6:** 3909–3916.

Casset, F., Imberty, A., Haser, R., Payan, F. & Perez, S. 1995. Molecular modelling of the interaction between the catalytic site of pig pancreatic α-amylase and amylose fragments. Eur. J. Biochem. **232:** 284–293.

Chen, Y., Fringant, C. & Rinaudo, M. 1997. Molecular characterization of starch by SEC: dependence of the performances on the amylopectin content. Carbohydr. Polymers **33:** 73–78.

Dygert, S., Li, L. H., Don Florida, R. & Thoma, J. A. 1965. Determination of reducing sugar with improved precision. Anal. Chem. **13:** 367–374.

Gilles, C., Astier, J.-P., Marchis-Mouren, G., Cambillau, C. & Payan, F. 1996. Crystal structure of pig pancreatic α-amylase isoenzyme II, in complex with the carbohydrate inhibitor acarbose. Eur. J. Biochem. **238:** 561–569.

Gottschalk, T. E., Fierobe, H. P., Mirgorodskaya, E., Clarke, A. J., Tull, D., Sigurskjold, B. W., Christensen, T., Payre, N., Frandsen, T. P., Juge, N., McGuire, K. A., Cottaz, S., Roepstorff, P., Driguez, H., Williamson, G. & Svensson, B. 1998. Structure, function and protein engineering of starch-degrading enzymes. Biochem. Soc. Trans. **26:** 198–204.

Granger, M., Abadie, B., Mazzei, Y. & Marchis-Mouren, G. 1975. Enzymatic activity of TNB blocked porcine pancreatic α-amylase. FEBS Lett. **50:** 276–278.

Janecek, S. 1994. Sequence similarities and evolutionary relationships of microbial, plant and animal α-amylases. Eur. J. Biochem. **224:** 519–524.

Jespersen, H. M., MacGregor, E. A., Sierks, M. R. & Svensson, B. 1991. Comparison of the domain-level organization of starch hydrolases and related enzymes. Biochem. J. **280:** 51–55.

King, E. L. & Altman, C. 1956. A schematic method of deriving the rate laws for enzyme catalyzed reactions.J. Phys. Chem. **60:** 1375–1378.

Kondo, H., Nakatani, H. & Hiromi, K. 1990. In vitro action of human and porcine α-amylases on cyclomalto-oligosaccharides. Carbohydr. Res. **204:** 207–213.

Koukiekolo, R., Le Berre-Anton, V., Desseaux, V., Moreau, Y., Rougé, P., Marchis-Mouren, G. & Santimone, M. 1999. The mechanism of porcine pancreatic α-amylase. Inhibition of amylose and maltopentaose hydrolysis by kidney bean (*Phaseolus vulgaris*) inhibitor and comparison with that by acarbose. Eur. J. Biochem. **265:** 20–26.

Koukiekolo, R., Desseaux, V., Moreau, Y., Marchis-Mouren, G. & Santimone, M. 2001. Mechanism of porcine pancreatic α-amylase. Inhibition of amylose and maltopentaose hydrolysis by α-, β- and γ-cyclodextrins. Eur. J. Biochem. **268:** 841–848.

Larson, S. B., Greenwood, A., Cascio, D., Day, J. & McPherson, A. 1994. Refined molecular structure of pig pancreatic α-amylase at 2.1 Å resolution. J. Mol. Biol. **235:** 1560–1584.

Le Berre-Anton, V., Bompard-Gilles, C., Payan, F. & Rougé, P. 1997. Characterization and functional properties of the α-amylase inhibitor (α-Ai) from kidney bean (*Phaseolus vulgaris*) seeds. Biochim. Biophys. Acta **1343:** 31–40.

McCarter, J. D. & Withers, S. G. 1994. Mechanisms of enzymatic glycoside hydrolysis. Curr. Opin. Struct. Biol. **4:** 885–892.

Nahoum, V., Roux, G., Anton, V., Rougé, P., Puigserver, A., Bischoff, H., Henrissat, B. & Payan, F. 2000. Crystal structures of human pancreatic α-amylase in complex with carbohydrate and proteinaceous inhibitors. Biochem. J. **346:** 201–208.

Pasero, L., Mazzei-Pierron, Y., Abadie, B., Chicheportiche, Y. & Marchis-Mouren, G. 1986. Complete amino acid sequence and location of the 5 disulphide bridges in porcine pancreatic α-amylase. Biochim. Biophys. Acta **869:** 147–157.

Qian, M., Haser, R., Buisson, G., Duée, E. & Payan, F. 1994. The active center of mammalian α-amylase. Structure of the complex of a pancreatic α-amylase with a carbohydrate inhibitor refined to 2.2 Å resolution. Biochemistry **33:** 6284–6294.

Qian, M., Haser, R. & Payan, F. 1993. Structure and molecular model refinement of pig pancreatic α-amylase at 2.1 Å resolution. J. Mol. Biol. **231:** 785–799.

Qian, M., Haser, R. & Payan, F. 1995. Carbohydrate binding sites in a pancreatic α-amylase-substrate complex, derived from X-ray structure analysis at 2.1-Å resolution. Protein Science **4:** 747–755.

Qian, M., Spinelli, S., Driguez, H. & Payan, F. 1997. Structure of a pancreatic α-amylase bound to a substrate analogue at 2.03 Å resolution. Protein Science **6:** 2285–2296.

Robyt, J. F & French, D. 1970. The action pattern of porcine pancreatic α-amylase in relationship to the substrate binding site of the enzyme. J. Biol. Chem. **245:** 3917–3927.

SAS Institute Inc. 1989. SAS/STAT® User's Guide, Version 6, Fourth edition, **1:** 943. Sas Institute Inc., Cary, NC, USA.

Received February 6, 2002
Accepted April 18, 2002